Applied Polymer
JOURNAL OF
SCIENCE

High Dielectric Constant Polyaniline/Sulfonated Poly(aryl ether ketone) Composite Membranes with Good Thermal and Mechanical Properties

Yunhe Zhang, Pengfei Huo, Xiao Liu, Changru Rong, Guibin Wang

Alan G. MacDiarmid Laboratory, College of Chemistry, Jilin University, Changchun 130012, People's Republic of China
Correspondence to: G. Wang (E-mail: wgb@jlu.edu.cn)

ABSTRACT: All-organic polyaniline (PANI)/sulfonated poly(aryl ether ketone) (SPAEK) composite membranes consisting of a PANI (conducting) filler evenly distributed in an SPAEK (insulating) matrix were prepared with a solution-blending technique. The dielectric properties, electrical conductivity, and thermal and mechanical performances of the all-organic PANI/SPAEK composite membranes were investigated as a function of different PANI loading levels. The composite membrane containing 30 wt % PANI exhibited a high dielectric constant of about 600, a low dielectric loss tangent of about 0.6 (at 1 kHz), and good thermal properties (temperature for 5% weight loss > 250°C) and mechanical properties (tensile strength ≈ 35 MPa). © 2013 Wiley Periodicals, Inc. J. Appl. Polym. Sci. 130: 1990–1995, 2013

INTRODUCTION

The past several decades have witnessed huge progress in the synthesis of polymeric films with high dielectric constants, low dielectric losses, and good thermal stability; this has been driven by their diverse applications in actuators, artificial muscles, charge-storage devices, inductors, resistors, and so on.[1–4] Recently, all-organic, high-dielectric-constant and low-dielectric-loss polymeric films have been widely investigated in the fabrication of embedded passives for their mechanical flexibility, low-temperature processability, and good process compatibility with printed circuit boards.[5,6] Among these polymeric films, conductive filler/polymer composites have gained special attention because they show a dramatic increase in their dielectric constants close to the percolation threshold. Until now, various metal fillers, such as silver, aluminum, and nickel, have been used to prepare metal/polymer composites or three-phase percolative composite films.[2,7–10] This material option represents advantageous characteristics over conventional ceramic/polymer composites, including an ultrahigh dielectric constant with balanced mechanical properties, including the adhesion strength. However, the major hurdles for this type of high dielectric constant composite include the low dielectric breakdown field and high dielectric loss inherent in these systems. To overcome these drawbacks, all-organic polymeric films consisting of conducting polymer particulates within a host polymer matrix with good mechanical strength, high thermal stability, and high dielectric breakdown field are of current interest.

Polyaniline (PANI), one of the most promising conducting polymers, has been investigated in the fabrication of PANI/polymer composite films for its high polymerization yield, controllable electrical conductivity, good environmental stability, and relatively low cost.[11–13] Additionally, the low concentration of PANI within polymeric composite films can endow the films with conductive or semiconductive capabilities and promote the development of thin, light, flexible, and inexpensive organic electronics in displays, sensors, solar technology, and proton-exchange membranes.[14–17]

In this study, an advanced all-organic composite consisting of PANI particles as a functional filler and sulfonated poly(aryl ether ketone) (SPAEK) as the polymer matrix was investigated. SPAEK was chosen in our experiment as the polymer matrix because of its special alternative structure of ether and ketone, which can enable composite films to possess good thermal and mechanical properties.[18] The influence of the PANI loading levels on the properties of the PANI/SPEAK composite films was investigated.

EXPERIMENTAL

Materials

Aniline was purchased from Aldrich. Bisphenol A, ammonium peroxydisulfate (APS), and sulfosalicylic acid (SSA) were purchased from Beijing Chemical Reagent. 4,4′-Difluorobenzophenone (DFBP) was purchased from Yianbian Chemical Factory and purified by recrystallization from a mixture of ethanol and
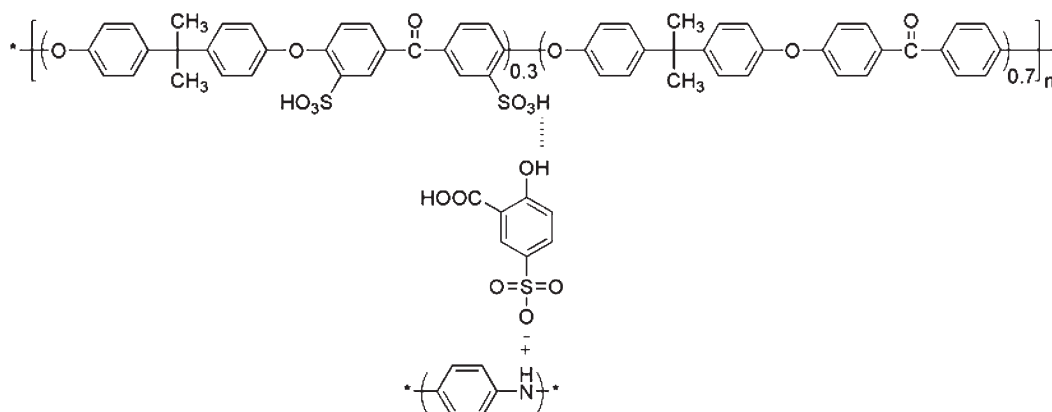
Scheme 1. Synthesis of the SPAEK copolymers and PANI/SPAEK composite membranes.

deionized water. K_2CO_3 (Beijing Chemical Reagent) was ground into fine powder and dried at 120°C for 24 h before polymerization. All of the organic solvents were obtained from commercial sources and purified by conventional methods. All aqueous solutions were prepared with deionized water.

Synthesis of SPAEK[19]

Sodium 5,5′-carbonylbis(2-fluorobenzenesulfonate) was synthesized by sulfonated DFBP with fuming sulfuric acid (50% SO_3); this was followed by neutralization with NaOH and NaCl. As shown in Scheme 1, poly(ether ether ketone)s were obtained by DFBP (0.07 mol), sodium 5,5′-carbonyl-bis(2-fluoroben-zenesulfonate) (0.03 mol), and bisphenol A(0.10 mol) via nucleophilic aromatic substitution with toluene to remove water formed

during the polycondensation. The polymer was transformed to acid form (SPAEK) by ion exchange in $2M$ H_2SO_4.

Polymerization of PANI–SSA

APS (0.l mol) was dissolved in 100 mL of aqueous HCl ($0.1M$) at room temperature (25 ± 2°C). Aniline (0.1 mol) was dispersed in 500 mL of aqueous HCl ($0.1M$) in a 2000-mL beaker with strong mechanical stirring for 0.5 h at room temperature. The APS solution was poured into the aniline suspension under strong stirring for 6 h. Then, the suspension was separated by centrifugation. The precipitate was collected and transferred into 500 mL of aqueous HCl ($0.1M$) under strong stirring for 1 h. After that, the suspension was separated by centrifugation and washed five times. The precipitate was dropped into
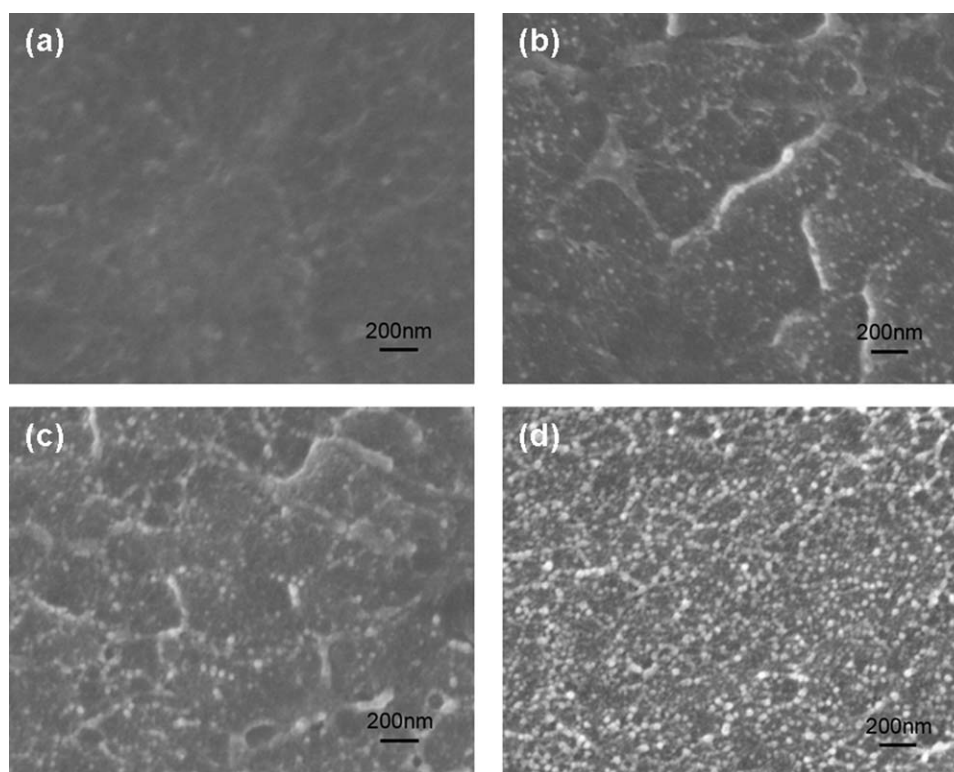

Figure 1. SEM micrographs of PANI/SPAEK composites with different PANI contents: (a) 10, (b) 20, (c) 30, and (d) 40 wt %.
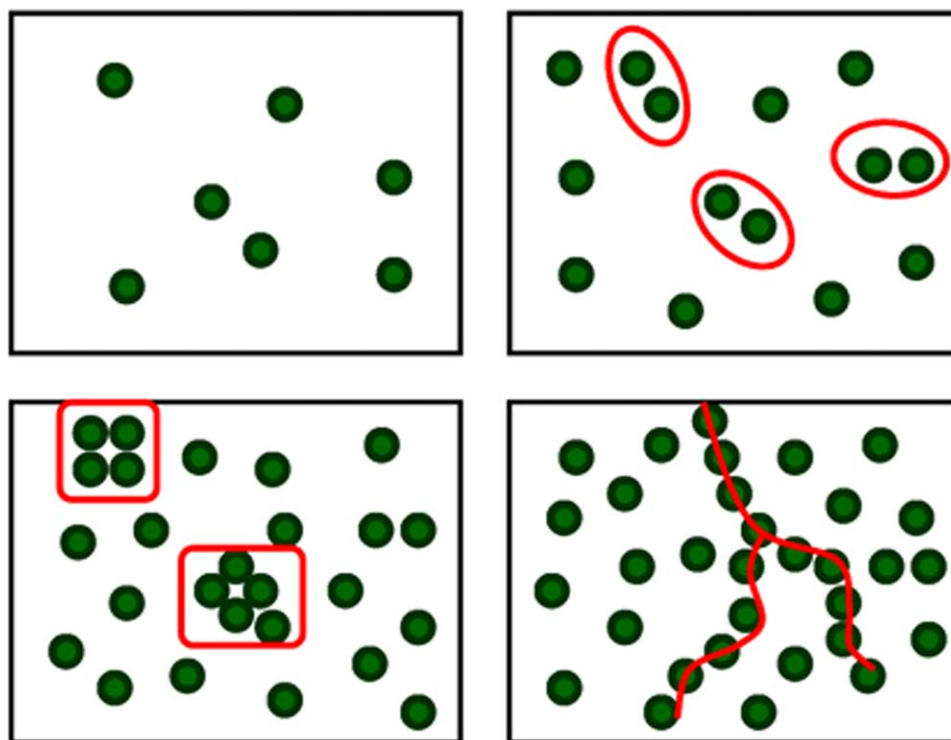
Figure 2. Schematic images of the microstructure of the PANI/SPAEK nanocomposite with different PANI contents. [Color figure can be viewed in the online issue, which is available at wileyonlinelibrary.com.]

aqueous ammonia hydroxide (0.1M) for 24 h at room temperature. Consequently, the products were dried in a dynamic vacuum for 48 h at room temperature. Finally, the precipitate was dispersed in an aqueous acidic medium (2M SSA) with mechanical stirring for 24 h at room temperature. The products were washed until they were neutral; then they were washed by ethanol and dried in a dynamic vacuum. Finally, the dark green PANI–SSA (where PANI refers to PANI–SSA later) was obtained.

Preparation of the PANI/SPAEK Composite Membranes
The composite films were prepared with the solution casting method. The PANI–SSA was ultrasonically dispersed in N-methylpyrrolidone (NMP) for 2 h to form a stable suspension. At the same time, SPAEK was also dissolved in NMP. Then, the suspension of PANI–SSA in NMP was added to the SPAEK solution, and the mixtures were subjected to ultrasonic treatment for 2 h and stirred for 12 h. The mixtures were then poured onto glass slides and dried in air at 60°C for 6 h and *in vacuo* at 60°C for 12 h. Finally, the PANI/SPAEK (where PANI/SPAEK refers to PANI–SSA/SPAEK in this article) composites were annealed at 110°C in a vacuum for 12 h and were slowly cooled to room temperature.

Instrumentation
The microstructures of the PANI/SPAEK composites were characterized with scanning electron microscopy (SEM; JEOLJSM-6700). To investigate the morphology of the composite, the sample was broken in liquid nitrogen, and its cross section was analyzed by SEM. For electrical measurements, electrodes were painted with silver paste. The dielectric response of the composites was measured with an Alph-A high-performance frequency analyzer in the frequency range 100–10^6 Hz.

RESULTS AND DISCUSSION

Figure 1 shows typical SEM images of PANI/SPAEK composite films with different PANI loading levels. From the SEM images, it can be clearly seen that when the PANI loading level was 10 wt %, no PANI fillers could be found. When the PANI loading level was increased to 20, 30, or 40 wt %, PANI particles with an average diameter about 40 nm evenly dispersed in the SPAEK matrix could be detected; this confirmed the good interphase interaction for the hydrogen-bonding interactions between the sulfonic groups of SPAEK and the hydroxyl groups of PANI, as shown in Scheme 1.

Because the conductive PANI fillers were separated by SPAEK insulation layers, the PANI fillers could be regarded as spherical particles with an average diameter of 40 nm. It is simple to consider a straightforward calculation of the average interparticle distance ($S_{average}$):[20,21]

$$S_{average} = d\left[\left(\frac{\pi}{6\varphi_v}\right)^{\frac{1}{3}} - 1\right] \quad (1)$$

where d is the diameter and φ_v is the volume fraction of PANI. In the PANI/SPAEK films, the thickness of the insulation layer between the PANI particles could be estimated according to this equation, in which the densities of SPAEK and PANI were 1.22 and 1.38 g/cm^3, respectively. When the PANI loading levels ranged from 10 to 20 wt %, the volume fraction of PANI

particles within the SPAEK matrix varied from 9 to 18 vol %. At this time, the values of s between adjacent conductive particles ranged from 40 to 17 nm; this effectively prohibited the occurrence of large leakage currents because only limited microcapacitors could form. This resulted in low dielectric constants in the corresponding hybrid films. When the PANI loading level was 30 wt % (27 vol %), the value of s was reduced to 10 nm; this implied a higher dielectric constant and acceptable dielectric loss tangent (tan δ) because of the formation of more microcapacitors. When the PANI loading level was 40 wt %, the value of s decreased further to 5 nm; thus, the conductive network was easily formed among the particles, and this resulted in even higher dielectric constant and tan δ values. All of the changes with various PANI loading levels are illustrated in Figure 2.

To further prove our hypothesis, the dielectric constant and tan δ as a functions of the PANI loading level were measured at room temperature and 10^3 Hz, as shown in Figure 3. Figure 3(a) displays the dielectric constant as a function of the PANI loading level. When the PANI loading levels were 10 and 20 wt %, the moderate dielectric constant increased from 18 to 50.
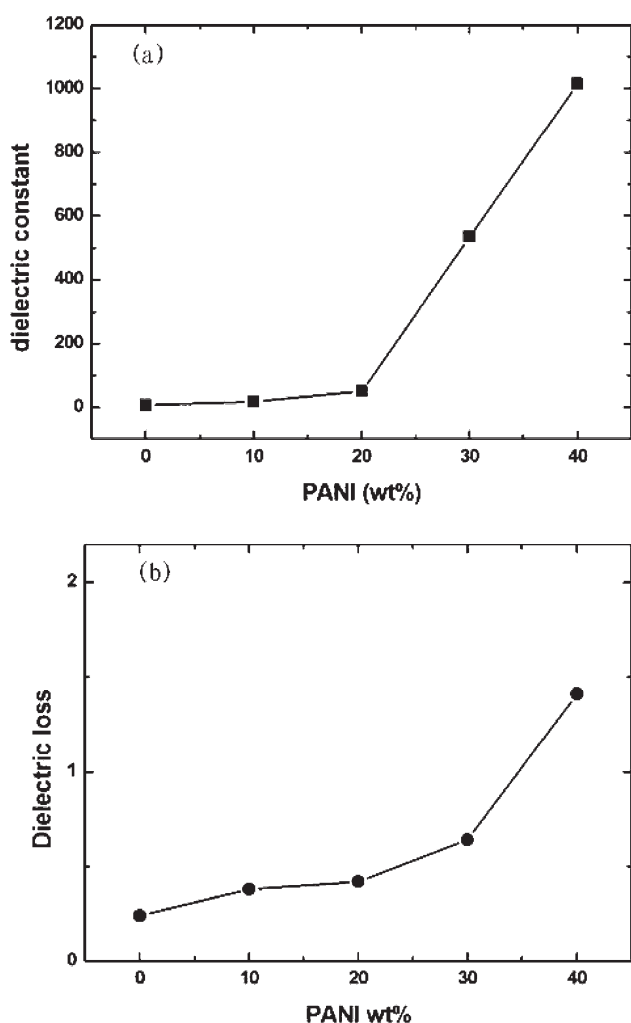

Figure 3. Dependence of the (a) dielectric constant and (b) tan δ with different PANI contents at room temperature and 10^3 Hz.
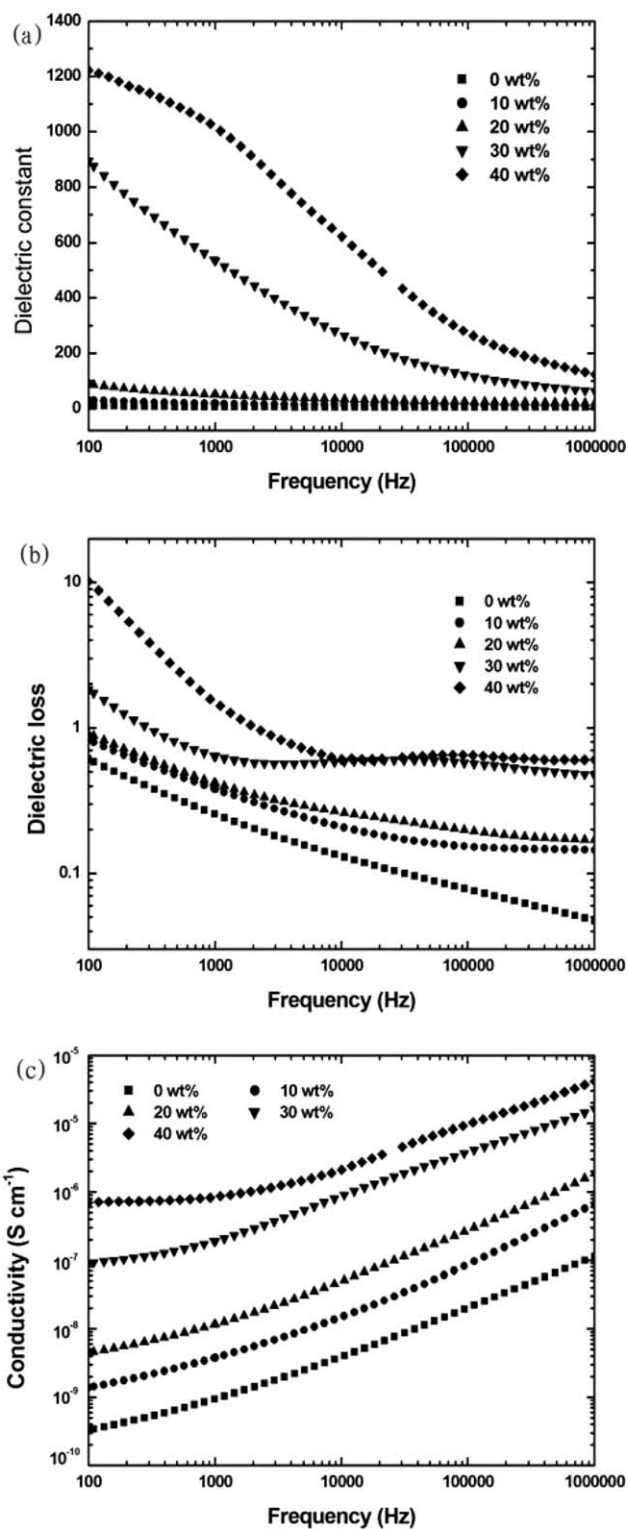

Figure 4. Dependence of the (a) dielectric constant, (b) tan δ, and (c) conductivity of the PANI/SPAEK with different PANI contents on the frequency, which ranged from 10^2 to 10^6 Hz, measured at room temperature.

When the PANI loading level was 30 wt %, a percolation phenomenon was observed, and the dielectric constant reached 534. When the PANI loading level was 40 wt %, the dielectric constant increased further to 1015. Figure 2(b) presents the

tan δ of the PANI/SPAEK films as a function of the PANI loading level. We observed that tan δ was less than 0.65 when the PANI loading level ranged from 0 to 30 wt % because of the relatively large distance between adjacent conductive particles, which could prohibit the occurrence of a large leakage current. However, when PANI loading level was increased to 40 wt %, tan δ was enhanced from 0.64 to 1.57 because a conductive network was easily formed among the adjacent particles. Consequently, the leakage current increased because the thickness of the insulation layer was only about 5 nm; this could not effectively prohibit the occurrence of a large leakage current. These results further prove our hypothesis. This series of composites had lower tan δ values than the PANI–DBSA/PAA composites,[22] and compared with carbon nanotube/SPAEK composites,[18] these composites had a high dielectric constant and lower tan δ as well. This was because the electrical conductivity of the semiconductor PANI was lower than that of carbon nanotubes, and organic-phase PANI exhibited a better dispersion than carbon nanotubes in the polymer matrix, which prevented an amount of electron accumulation.

The dielectric properties of the composites for different PANI contents are shown in Figure 4. The dielectric constant [Figure 4(a)] increased slowly with increasing PANI when the PANI contents were 10 and 20 wt %, whereas it decreased with increasing frequency. The dielectric constant increased sharply to 890 at 100 Hz when the PANI content was 30 wt %; this was nearly 100 times higher than that of the pure SPAEK matrix. As indicated by the SEM micrograph described previously, the majority of the nanosized PANI particles were well dispersed in the SPAEK matrix. These well-dispersed nanosized PANI particles served as minicapacitors within the composites. Thus, the high dielectric constant of the PANI/SPAEK composite material was attributed to the accumulation of these nanosize capacitors. Because these nanosize particles were embedded within the SPAEK matrix, the charge associated with the individual particles was localized to those particles and could not jump to adjacent particles. Figure 4(b) displays the variation of the dielectric tangent with the PANI content. It shows that tan δ
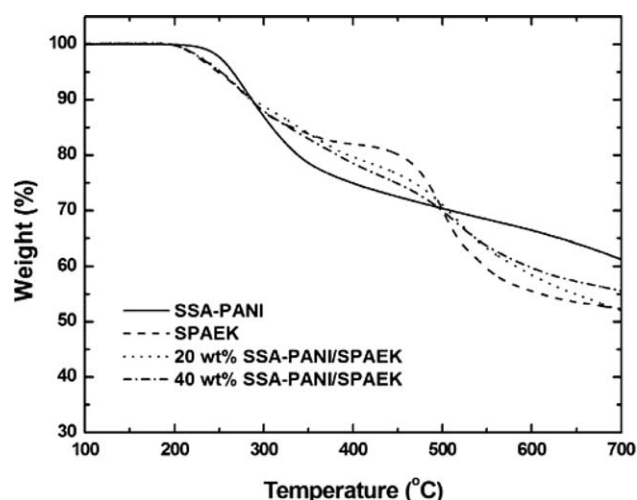
Table I. Mechanical Properties of the PANI/SPAEK Composites

Sample	Tensile strength (MPa)	Tensile modulus (GPa)	Elongation at breakage (%)
SPAEK	26.8	1.1	98.8
SPAEK/10% PANI	48.9	2.2	45.9
SPAEK/20% PANI	45.0	2.4	17.7
SPAEK/30% PANI	34.2	2.8	4.5
SPAEK/40% PANI	—	—	—

decreased gradually with frequency for the composites. The tan δ value of the composites was enhanced with increasing PANI content. When the PANI content was lower (<30 wt %), tan δ was less than 1. Figure 4(c) shows the conductivity of the PANI/SPAEK composites as a function of the frequency with different PANI contents. When the PANI contents were 0–20 wt %, the conductivity of the composites increased almost linearly with increasing frequency. When the PANI contents were 30 and 40 wt %, the conductivity value was almost independent of the change of frequency within a low-frequency range.

The thermal stability behavior of the neat PANI, SPAEK, and PANI/SPAEK composites with different PANI contents are shown in Figure 5. The temperature for the 5% weight loss of the composites was over 250°C; this showed excellent thermal stability for the PANI/SPAEK composites. The thermogravimetric analysis curves of the SPAEK and PANI/SPAEK composites exhibited two distinct thermal degradation steps. The first weight loss step was associated with the loss of sulfonic groups, whereas the second observed weight loss was due to main-chain degradation.

The mechanical properties of the PANI/SPAEK composites are shown in Table I. The SPAEK/PANI 10% and SPAEK/PANI 20% had tensile strengths of 48.9 and 45.0 MPa and tensile moduli of 2.2 and 2.4 GPa, which were much higher than those of pure SPAEK (26.8 MPa and 1.1 GPa, respectively). The composite with the PANI mass fraction of 0.40 had a tensile strength of 24.2 MPa, which was lower than that of SAPEK. The elongations at break of SPAEK/PANI 10%, SPAEK/PANI 20%, and SPAEK/PANI 30% were 45.9, 17.7, and 3.5%, respectively; these values were lower than that of SPAEK (98.8%). At low PANI contents, the tensile strength of these composites increased, and this was attributed to two factors: (1) the good interphase interaction for the hydrogen-bonding interactions between the sulfonic groups of SPAEK and the hydroxyl groups of PANI, which immobilized or partially immobilized the polymer phases and added stiffness to the composite layers, and (2) the high aspect ratio and surface area of the PANI. When the PANI content in the composites was increased further, the tensile strength of the composites decreased because of the inevitable aggregation of PANI at higher PANI contents.

Figure 5. Thermogravimetric analysis curves of the PANI/SPAEK composite.

CONCLUSIONS

In summary, we prepared novel two-phase all-organic PANI/SPAEK nanocomposites with high dielectric constants, low

dielectric losses, and good thermal and mechanical properties with a simple solution-blending technique. The influence of the PANI loading levels on the morphological, dielectric, electrical, and thermal and mechanical properties of the composites was investigated. SEM micrographs revealed that the PANI particulates dispersed well in the SPAEK matrix because of the hydrogen-bonding interactions between the sulfonic groups of SPAEK and the hydroxyl groups of PANI. The dielectric behaviors of the composite were determined by the PANI loading levels for the formation of microcapacitors between adjacent PANI fillers. Moreover, excellent thermal stability and mechanical performance in the PANI/SPAEK composites were also obtained. Those outstanding performances make our samples suitable for applications in capacitors and inductors devices.

ACKNOWLEDGMENTS

REFERENCES

1. Zhang, Q. M.; Li, H. F.; Poh, M.; Xia, F.; Xu, H. S. *Nature* **2002**, *419*, 284.

2. Dang, Z. M.; Lin, Y. H.; Nan, C. W. *Adv. Mater.* **2003**, *15*, 1625.

3. Daisuke, N.; Takafumi, K.; Akira, W.; Mikio, K. *Polym. Int.* **2011**, *60*, 1180.

4. Xu, H.; Bai, Y.; Bharti, V.; Cheng, Z. Y. *J. Appl. Polym. Sci.* **2001**, *82*, 70.

5. Gregorio, R.; Cestari, J. M.; Bernardino, F. E. *J. Mater. Sci.* **1996**, *31*, 2925.

6. Rao, Y.; Yue, J.; Wong, C. P. *Electr. Compos.* **2002**, *25*, 123.

7. Huang, X. G.; Jiang, P. K.; Kim, C.; Ke, Q. Q.; Wang, G. L. *Compos. Sci. Technol.* **2008**, *68*, 2134.

8. Panda. M.; Srinivas, V.; Thakur, A. K. *Appl. Phys. Lett.* **2008**, *92*, 132905.

9. Qi, L.; Lee, I.; Chen, S. H.; Samuels, W. D.; Exarhos, G. *J. Adv. Mater.* **2005**, *17*, 1777.

10. Yang, X.; Wang, Q. T.; Zhang, Y. H.; Jiang, Z. H. *Polym. J.* **2012**, *44*, 1042.

11. Tsotra, P. O.; Friedrich, K. *Synth. Met.* **2004**, *143*, 237.

12. Tsotra, P. O.; Friedrich, K. *Chem. Phys.* **2005**, *206*, 787.

13. Chwang, C. P.; Liu, C. D.; Huang, S. W.; Chao, D. Y.; Lee, S. N. *Synth. Met.* **2004**, *142*, 275.

14. Moreira, V. X.; Garcia, F. G.; Soares, B. G. *J. Appl. Polym. Sci.* **2006**, *100*, 4059.

15. Huang, C.; Zhang, Q. M.; Su, *J. Appl. Phys. Lett.* **2003**, *82*, 3502.

16. Jang, J.; Bae, J.; Lee, K. *Polymer* **2005**, *46*, 3677.

17. Nagarale, R. K.; Gohil, G. S.; Shahi, V. K. *J. Membr. Sci.* **2006**, *280*, 389.

18. Liu, X.; Zhang, Y. H.; Zhu, M.; Yang, X.; Rong, C. R.; Wang, G. B. *Soft Mater.* **2011**, *9*, 94.

19. Wang, F.; Chen, T. L.; Xu, J. P. *Macromol. Chem. Phys.* **1998**, *199*, 1421.

20. Huang, C.; Zhang, Q. M. *Adv. Funct. Mater.* **2004**, *14*, 501.

21. Yuan, J. K.; Dang, Z. M.; Yao, S. H.; Zha, J. W.; Zhou, T.; Li, S. T.; Bai, J. B. *J. Mater. Chem.* **2010**, *20*, 2441.

22. Ho, C. H.; Liu, C. D.; Hsieh, C. H.; Hsieh, K. H.; Lee, S. N. *Synth. Met.* **2008**, *158*, 630.